ELSEVIER

Chemical Engineering Journal 67 (1997) 9–18

Chemical Engineering Journal

Modelling the performance of venturi scrubbers

R.A. Pulley *

Department of Chemical Engineering, Nottingham University, University Park, Nottingham NG7 2RD, UK

Received 3 June 1995; accepted 27 January 1997

Abstract

The performance of venturi scrubbers is expressed in terms of the pressure drop and dust collection efficiency. The model of Azzopardi et al. (Trans. Inst. Chem. Eng. 69 (1991) 237) which incorporates many of the phenomena of gas–liquid flow in the venturi has been extended in this work to include dust removal prediction based on inertial collection. Pressure drop and dust removal predictions of this and previous models are compared to extensive data for the two main types of venturi with either liquid injection at the throat or a wetted approach. The results show the current model gives significantly improved predictions compared with previous models over a wide range of venturi sizes and operating conditions. The effect of uncertainty in the major model parameters are investigated to identify the requirements for further work in this area. © 1997 Elsevier Science S.A.

Keywords: Venturi scrubbers; Gas cleaning; Particle collection

1. Introduction

Venturi wet scrubbers find applications in removal of particulate matter from gas streams such as downstream of solid fuel combustors. In the venturi the gas and particles are accelerated through the throat and liquid injected into the gas stream, the high relative velocity between drop and particle means high collection efficiencies can be achieved for small particle sizes. The particle collection performance is achieved at the expense of pressure drop through the venturi and the accurate prediction of pressure drop and collection efficiency is vital to the optimal design of these systems to achieve required environmental standards.

Two alternative types of venturi are in common use: (a) the wetted approach type where liquid is introduced onto the walls before the convergence and (b) where liquid is injected through nozzles into the throat. In the wetted approach type drops are formed due to the gas shear on the liquid film, particularly in the high velocity throat region, although a portion of the liquid remains as a film on the walls. The injection of liquid into the throat in the second type ensures high atomization into the gas stream but at the expense of having to maintain the spray system.

In this paper, following the initial work of Teixeira et al. [1], the venturi model of Azzopardi et al. [2] is extended to incorporate particle collection prediction and validated against extensive pressure drop and particle collection data for wetted approach type of venturi scrubber from Rudnick et al. [3] and for throat injection type from Yung et al. [4]. Comparison is also made with the predictions of pressure drop and collection efficiency for venturi scrubbers using the models of Ripperger and Dau [5], Yung [6] and Boll [7]. All experimental data from the above studies use air as the gas and water as the scrubbing liquid.

2. Venturi scrubber models

The performance of a venturi scrubber is specified in terms of the pressure drop and particle collection efficiency.

2.1. Pressure drop predictions

Azzopardi et al. [2] have shown their model (see Appendix A) to give superior predictions of pressure drop through venturi scrubbers particularly in the divergence region of the venturi where pressure recovery occurs. The model uses the one-dimensional model of Azzopardi and Govan [8] in the convergence and throat (where this produced good predictions of pressure drop) and a boundary-layer model in the diffuser section which incorporates growth of the boundary layer and separation of the flow. The two-phase region of the venturi is divided into small sections and

* Tel.: +44 115 9514176; fax: +44 115 9514181; e-mail: richard.pulley@nott.ac.uk

PII S1385-8947(97)00014-4

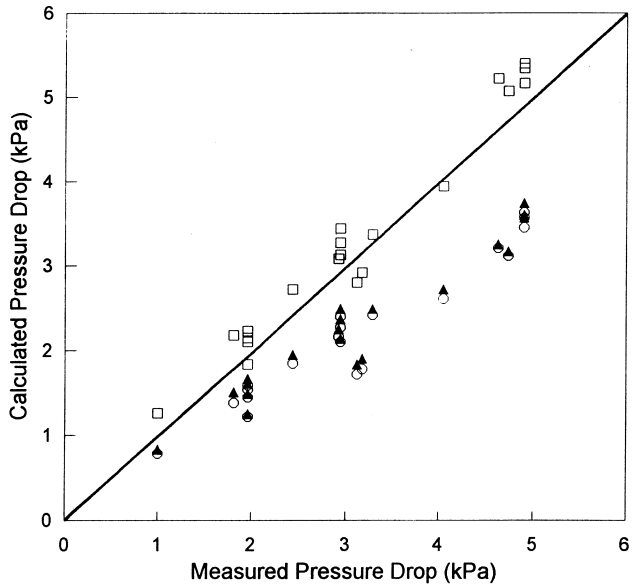

Fig. 1. Comparison of pressure drop predictions with data of Yung et al. [6] (see Section 2.1 for experimental details). □ Azzopardi et al. [2], ○ Boll [7], ▲ Ripperger and Dau [5].

entrainment from the liquid film in each section forms a group of droplets of a given size. The velocity and flow of each group of droplets are calculated along the venturi taking into account deposition of droplets from the gas to the liquid film. The method of predicting drop size is discussed in Section 2.2 with regard to particle collection.

Fig. 1 shows the comparison of pressure drop predictions from the Azzopardi et al. [2] model with the data of Yung et al. [4] for a venturi with liquid injection at the throat. Pressure drop predictions from the models of Boll [7] and Ripperger and Dau [6] are presented for comparison. The test venturi had a throat diameter of 0.078 m and four throat lengths from 0.12 to 0.58 m. The inlet and outlet pipe was 0.2 m inside diameter, convergence length was 0.28 m and the divergence was 0.5 m long. Operating conditions ranged from 32 to 71 m/s throat velocity and volumetric liquid to gas flow rate ratios of 1 to 3.3 l/m^3.

Fig. 2(a) and (b) show the comparison with the data of Rudnick et al. [3] for a wetted approach venturi, again predictions from the other models above are included. Three test venturis were used with dimensions shown in Table 1. Throat gas velocities ranged from 20 to 161 m/s and volumetric liquid to gas flow rate ratios from 0.2 to 3.7 l/m^3.

The test data therefore represents a severe test of the model over a wide range of geometries and conditions. The results show that the model of Azzopardi et al. [2] gives good prediction of pressure drop over the whole range of data with a consistent small overestimation. The other models, although giving better predictions under certain conditions, were not as consistent, particularly at higher pressure drops.

2.2. Particle collection

The model of Azzopardi et al. [2] is now extended to estimate the particle collection, and hence the particle concentration, along the venturi (hereinafter referred to as the 'current model'). The method uses the size and velocity of each droplet group already calculated for pressure drop prediction.

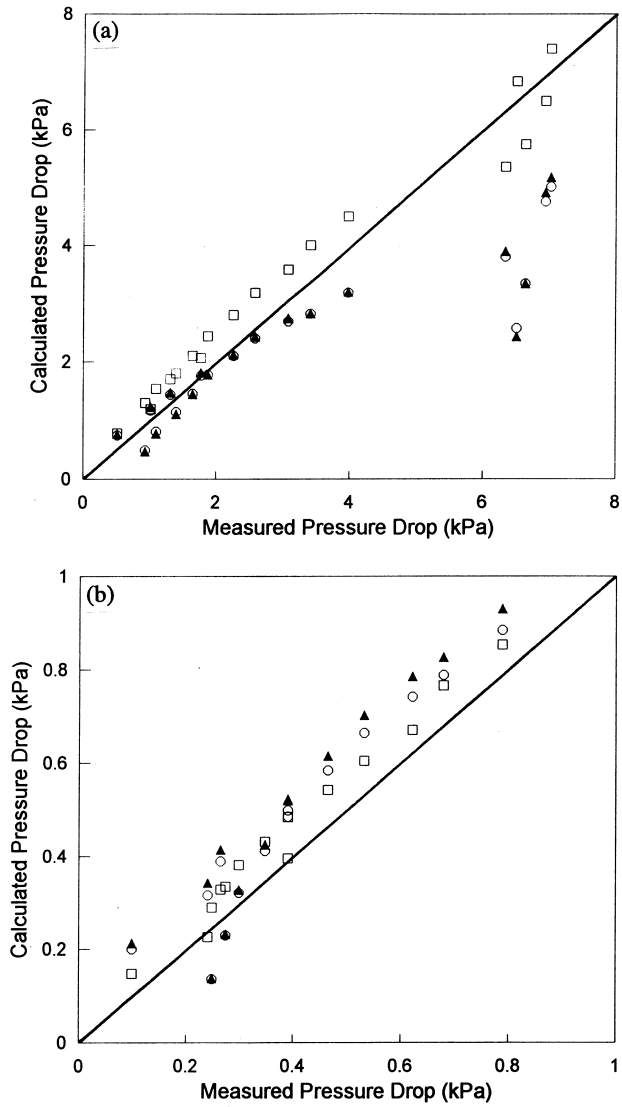

Fig. 2. Comparison of pressure drop predictions with data of Rudnick et al. [3] (see Section 2.1 for experimental details). □ Azzopardi et al. [2], ○ Boll [7], ▲ Ripperger and Dau [5]. (a) Data for 0.032 m and 0.054 m venturi throat diameters, and (b) data for 0.076 m venturi throat diameters.

The particle concentration is obtained from a material balance on the dust over a small increment of venturi length which leads to the following equation [9]:

$$-\frac{dc}{dz}=\frac{1.5\eta W_E u c \rho_g}{W_g D \nu_D \rho_l} \quad (1)$$

The contribution to the particle collection of each droplet group is calculated from Eq. (1), summed together, and the differential equation integrated numerically with the other model equations.

Table 1
Venturi dimensions from Rudnick et al. [3]

Venturi	Inlet/outlet pipe diameter (m)	Convergence length (m)	Throat length/diameter (m)	Divergence length (m)
Small	0.127	0.251	0.032/0.032	0.556
Medium	0.127	0.203	0.051/0.054	0.435
Large	0.127	0.138	0.076/0.076	0.305

2.2.1. Prediction of inertial drop collection efficiency

The prediction of collection efficiency (η) of drops in each group is based on the inertial impaction mechanism only. The calculations by Langmuir [10] of particle trajectories around spheres in potential and viscous flow fields have been confirmed by later investigators ([11,12]). Inertial collection is characterised by the dimensionless Stokes number (Stk) which is defined as:

$$\mathrm{Stk} = \frac{C_c \rho_p d^2 u}{9 \mu D} \tag{2}$$

The impaction parameter, usually defined as Stk/2, is also used.

Langmuir [10] presented his results in the form of correlations and it is convenient to use these in the model.

For potential flow around a spherical drop (drop Reynolds number $\mathrm{Re_D} \to \infty$):

$$\eta_p = \frac{\mathrm{Stk}^2}{(\mathrm{Stk}+0.5)^2} \tag{3}$$

For viscous flow ($\mathrm{Re_D} \to 0$):

$$\eta_v = \left[1 + \frac{0.75 \ln(2\mathrm{Stk})}{(\mathrm{Stk}-1.214)}\right]^{-2} \tag{4}$$

In most applications it is possible to select a flow field which is appropriate to the situation, for example in a spray tower the drops quickly accelerate to high Reynolds numbers relative to the gas and the potential flow equation is used. In the venturi scrubber the drops initially have a high relative velocity to the gas but are then accelerated towards gas velocity and in the diffuser can overtake the gas to provide additional collection of dust. The flow field therefore changes as the drop passes through the venturi. Langmuir [10] suggested an interpolation formula for the transition between viscous and potential flow to estimate the collection efficiency due to inertial impaction:

$$\eta_i = \frac{[\eta_v + \eta_p(\mathrm{Re_D}/60)]}{[1 + (\mathrm{Re_D}/60)]} \tag{5}$$

This equation assumes that the collection efficiency is the arithmetic mean of η_p and η_v at a Reynolds number of 60. This figure was chosen because it was noticed that on a log–log plot of drop size against terminal velocity, the straight line asymptotes at each end of the curve intersect at this point. Langmuir proposed that the collection efficiencies would behave in the same way. Herne [11] had this to say about the interpolation: ''Eq. (5)…may well have an element of truth in it, but it is quite impossible to justify it rigorously.'' When only considering dust collection in the throat use of the potential flow equation for collection efficiency is justifiable as the relative velocities in this region are high. However this work estimates collection throughout the venturi and consideration of different flow fields is required so Eq. (5) is used. It is shown below that there can be significant collection in the diffuser section of the venturi.

2.2.2. Interception collection

In the absence of electrostatic fields the other major collection mechanism that may be significant for particles of around 1 μm diameter is interception due to the size of the particle bringing it into contact with the collecting drop even though its centre, as predicted by the inertial collection mechanism, is outside the area collected. Compensation of the drop collection efficiency for interception was built into the current model using the method developed by Pulley and Walters [12]. Results from the model indicate that interception has a small effect (up to 2%) on the predicted overall dust removal in the venturi and this is considered insignificant compared to the overall accuracy of the model. To reduce the computational load of the model, the results presented here use the droplet collection efficiency calculation based on the inertial mechanism only.

2.2.3. Alternative venturi models

Results from the extended venturi model of Azzopardi et al. [2] are compared with two earlier models by Yung [6] and Boll [7] that predict dust collection.

The Yung model [6], developed from the previous work of Calvert [9], only considers collection to take place in the throat of the venturi and assumed the liquid is atomised at injection into monosized droplets. Yung's model [6] is in the form of a single equation for penetration (the fraction of particles entering the venturi that are not removed). It uses the equation of Walton and Woolcock [13] to predict the drop collection efficiency which is similar to Eq. (2) and was fitted to their experimental data.

Boll's model [7] assumes complete liquid atomization at injection but considers particle collection along all of the venturi. His original model predicted drop collection efficiency using theoretical calculations based on potential flow around the collector, however any method of prediction could be used with the basic venturi model equations describing gas and liquid drop dynamics. Therefore, to give a better comparison between the models, the method of calculating

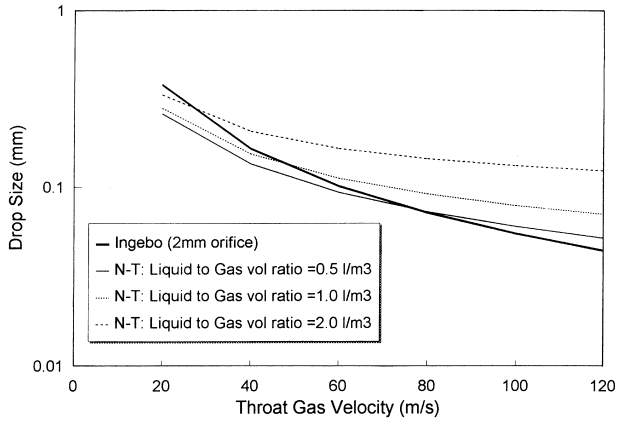

Fig. 3. Comparison of dropsize correlations. Ingebo [15] and Nukiyama and Tanasawa (N–T) [14] fluid properties for air/water system.

the drop collection efficiency given in Section 2.2.1 is used in Boll's model.

Both models are intended primarily to model venturis with liquid injection at the throat as they do not account for any significant liquid flowing on the walls.

2.2.4. Prediction of drop sizes

An important parameter in predicting the dust collection is the drop size generated in the venturi. Yung and Boll both use the Nukiyama and Tanasawa [14] correlation to predict a single drop size for the liquid injected. Where liquid is injected into the venturi throat this model of the process is reasonable, however, in the wetted approach type of venturi, atomization due to entrainment from the liquid film takes place all along the venturi and so this assumption is less valid. In the Azzopardi model, when liquid is injected into the throat the correlation of Ingebo [15] (Eq. (6)) is considered more appropriate and for drops produced by the shearing action of the gas on the wall film an equation suggested by Azzopardi [16] (Eq. (7)) derived from data for annular two-phase flow in vertical pipes is used:

$$D = 37D_{\mathrm{o}}(\mathrm{WeRe})^{-0.4} \tag{6}$$

$$D = 5.4\lambda \mathrm{We}_{\mathrm{m}}^{-0.58} + \frac{3.5\lambda\rho_{\mathrm{g}}W_{\mathrm{E}}}{\rho_{\mathrm{l}}W_{\mathrm{g}}} \tag{7}$$

Fig. 3 gives a comparison of the drop size predictions from the two correlations used for throat atomization. The Ingebo correlation is calculated for a 2 mm orifice, the Nukiyama and Tanasawa correlation is independent of orifice size but includes the liquid to gas volumetric flowrate ratio. The two predictions are comparable at lower throat velocities but deviate significantly at high velocities and large liquid to gas volumetric ratios.

3. Results

Comparison of model and experimental results is shown in two ways for each type of venturi in Figs. 4 and 5 for the data of Yung et al. [4] (throat injection) and Figs. 6 and 7 for the data of Rudnick et al. [3] (wetted approach). In each case measured and predicted particle penetration are plotted against each other for all available data, then penetration is plotted against particle size for a selection of experimental conditions. A statistical measure of the overall fit of each model is calculated based on the mean squared error from the experimental data.

3.1. Venturi with liquid injection at throat

Fig. 4(a)–(c) show the particle collection predictions of the current and earlier models outlined above, with the data of Yung et al. [4], 58 measurements in total. Fig. 5(a)–(d) show the comparison of models for a range of throat lengths and gas and liquid flows The data refers to a venturi scrubber with water injection at the throat removing fly ash particles from air (see Section 2.1 for more details). The superior prediction of particle collection by the current model, evident from the figures, is confirmed by looking at the mean squared error values: current model, 0.651; Boll's model, 2.02; Yung's model, 1.07.

With liquid injection at the throat the majority of the collection takes place in this section, examination of predicted dust concentration profiles in the venturi using the current model indicates that at least 95% of the collection is in the

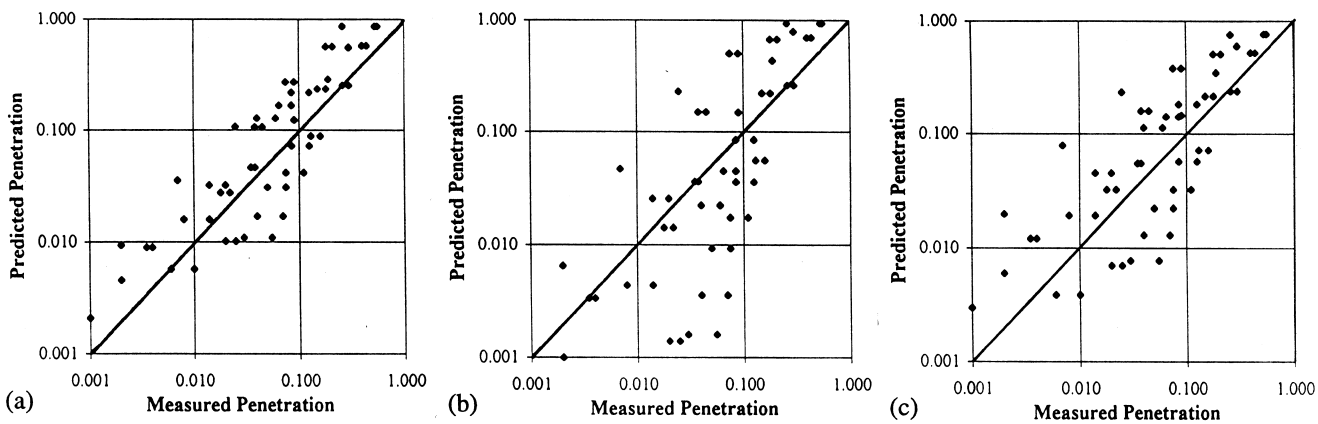

Fig. 4. Model predictions of particle penetration data from Yung et al. [4] for venturis with liquid injection at throat. (a) Current model, (b) Boll's model, and (c) Yung's model.

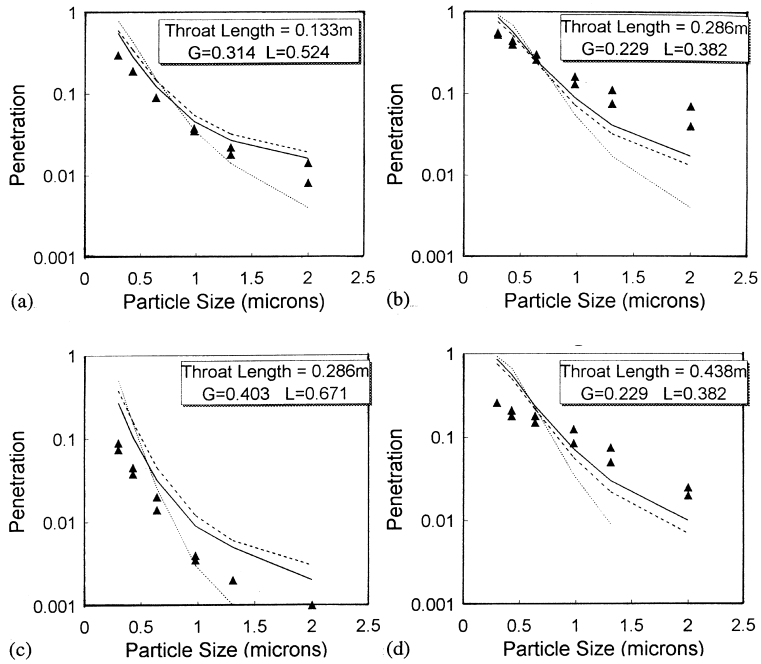

Fig. 5. Model predictions of particle penetration data from Yung et al. [4] for venturis with liquid injection at throat. Air (G) and water (L) flows in kg/s. ———— Current model, - - - Yung [6]. ····· Boll [7].

throat due to the drops formed where the liquid enters. The model of Yung et al. [6] assumes all collection is in the throat and so the penetration predictions are similar, the differences being mainly due to the method of calculating drop velocities.

3.2. Venturi with wetted approach

Rudnick et al. [3] presented extensive data for the wetted approach venturis specified in Table 1 and a range of air (G) and water (L) flow rates. The particles in this case were atomised cooking oil. Fig. 6(a)–(c) show the comparison for the three models with 790 measurements of particle penetration. In addition groups of data have been selected that represent a wide range of operating conditions for the three venturi configurations to thoroughly test the models' performance and the results are presented in Fig. 7(a)–(i). Again the current model appears to give more consistent predictions of penetration with a consistent over prediction in most cases. The poorest results in both Figs. 6 and 7 are for data from the venturi with the small throat diameter. The goodness of fit is confirmed by the mean squared error values: current model, 0.186; Boll's model, 0.485; Yung's model, 0.280.

Errors in the experimental data presented by Rudnick et al. [3] are indicated to be of the order of $\pm 50\%$ when the penetration is as low as 0.1 (i.e. small concentrations of particles in the exit gas). Values of penetration greater than 1.0 at small particle sizes also show the difficulty in accurate measurement of dust concentration.

The current model predicts significant collection taking place in the convergence and diffuser as well as the throat for the wetted approach configuration. For the range of condi-

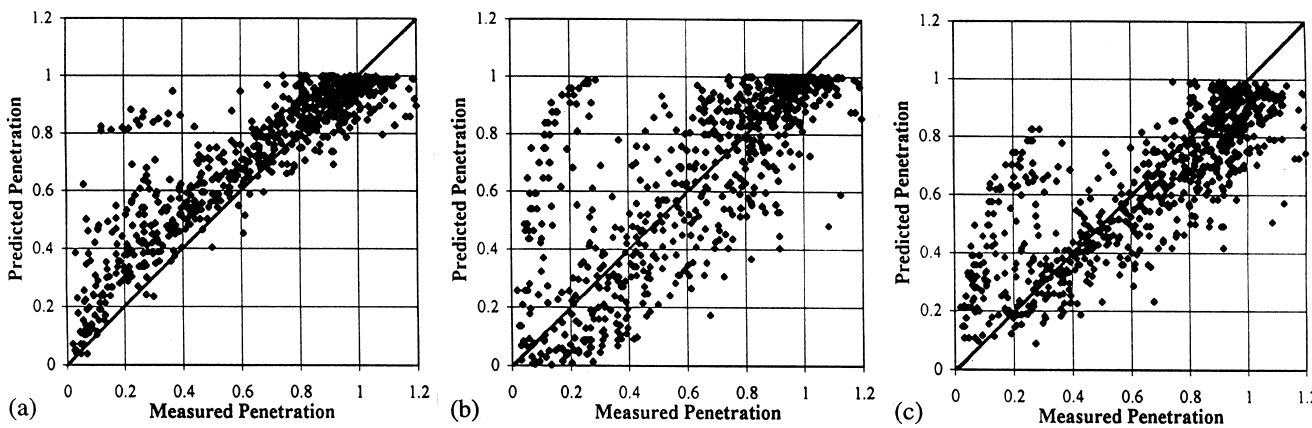

Fig. 6. Model predictions of particle penetration data from Rudnick et al. [3] for wetted approach venturis. (a) Current model; (b) Boll's model; (c) Yung's model.

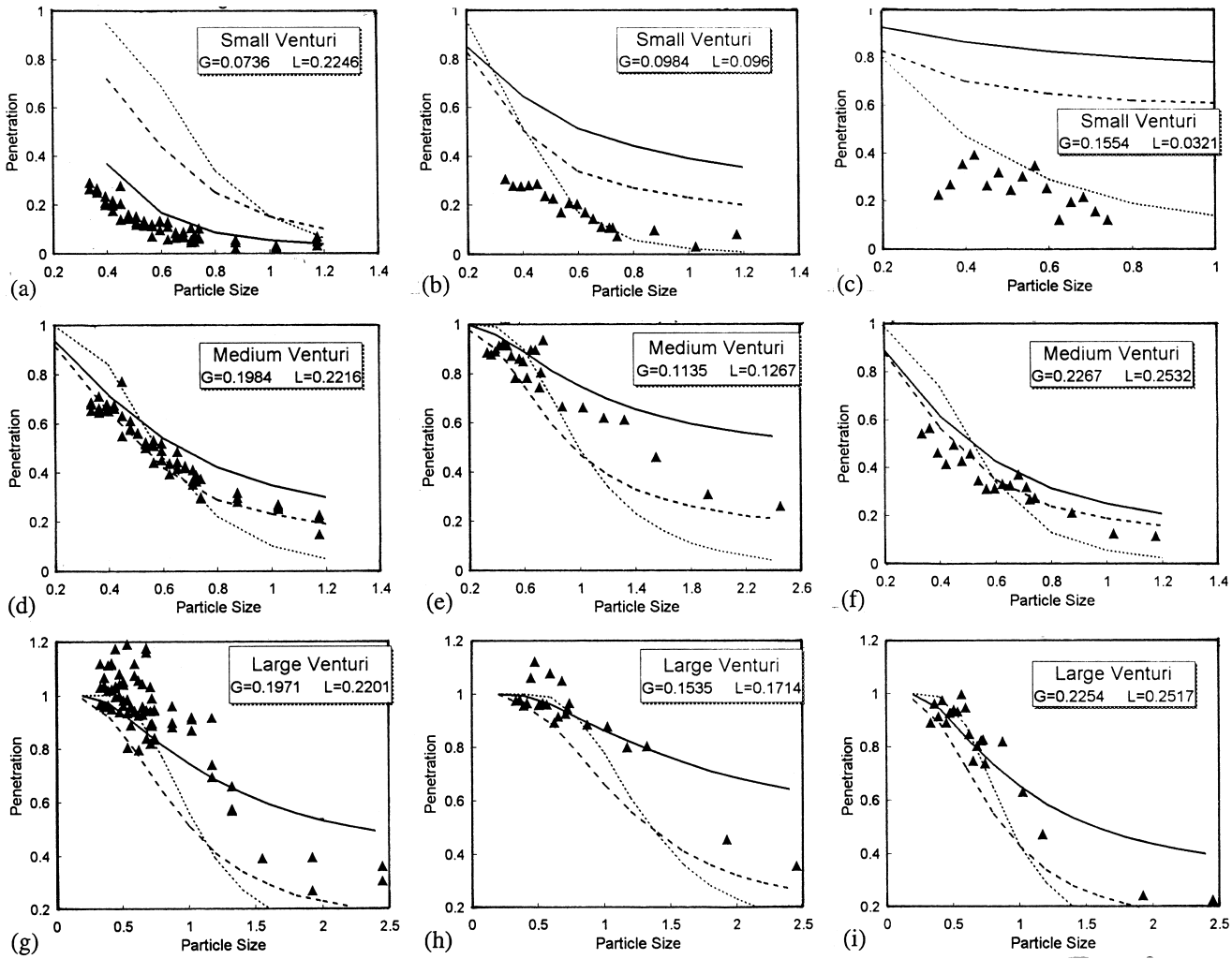

Fig. 7. Model predictions of particle penetration. Data from Rudnick et al. [3] for wetted approach venturis (see Table 1) Particle sizes in microns. Air (G) and water (L) flows in kg/s. ———— Current model, ····· Boll [7], - - - Yung [6].

tions examined, although over 70% of the collection has taken place by the end of the throat, up to 40% can take place in the convergence, particularly for larger dust particle sizes. The larger the venturi throat the greater the proportion of the collection that takes place in the diffuser and less in the convergence and throat.

Overall the results show that the current model, presented here, gives superior predictions of particle collection to previous models and, because it is more fundamentally based on the phenomena occurring in the venturi, it should be superior for extrapolation to industrial size equipment for design purposes. It should be noted that the parameters in the model, such as entrainment and deposition rates and drop size correlations, have not been adjusted to improve the model fit. At present these are based on other geometries such as annular flow in pipes, hence there is scope for further tuning of these factors as data becomes available.

4. Model parameter sensitivity

The effect of uncertainty in the major model parameters have been examined for each type of venturi. Fig. 8(a)–(c) show the change in predicted penetration for venturis with liquid injection at the throat, the experimental conditions and data are the same as Fig. 5(b). In Fig. 8(a) the drop size predicted by the correlation by Ingebo [15] is changed by $\pm 50\%$, a decrease in drop size created at injection producing a significant increase in the dust collected (decrease in penetration) due to the smaller drops having a higher collection efficiency. Fig. 8(b) indicates that the dust collection is relatively insensitive to the rate of deposition of liquid from the gas to the wall. It is normally assumed that all the liquid injected is atomised at the injection point, Fig. 8(c) shows how the collection is reduced if not all liquid is entrained.

Fig. 9(a)–(c) show the change in predicted penetration for the wetted approach type venturi, experimental conditions and data are the same as for Fig. 7(d). Fig. 9(a) and (b) show the effect of changing the drop size and initial velocity to be small. The drops in this case are generated all along the venturi by entrainment from the wall film and their size is predicted from the correlation of Azzopardi [16]. As before a smaller drop size gives an increase in dust collection. The initial velocity of the drops formed from the wall film is set

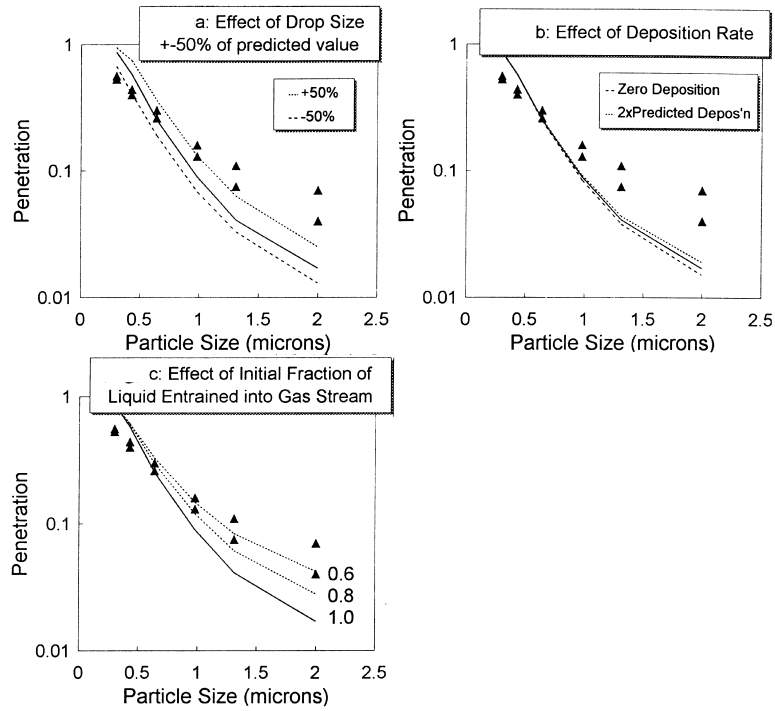

Fig. 8. Effect of model parameters on particle penetration data for venturi with liquid injection at throat from Yung et al. [4]. Throat length = 0.286 m, gas flow = 0.229 kg/s, liquid flow = 0.382 kg/s.

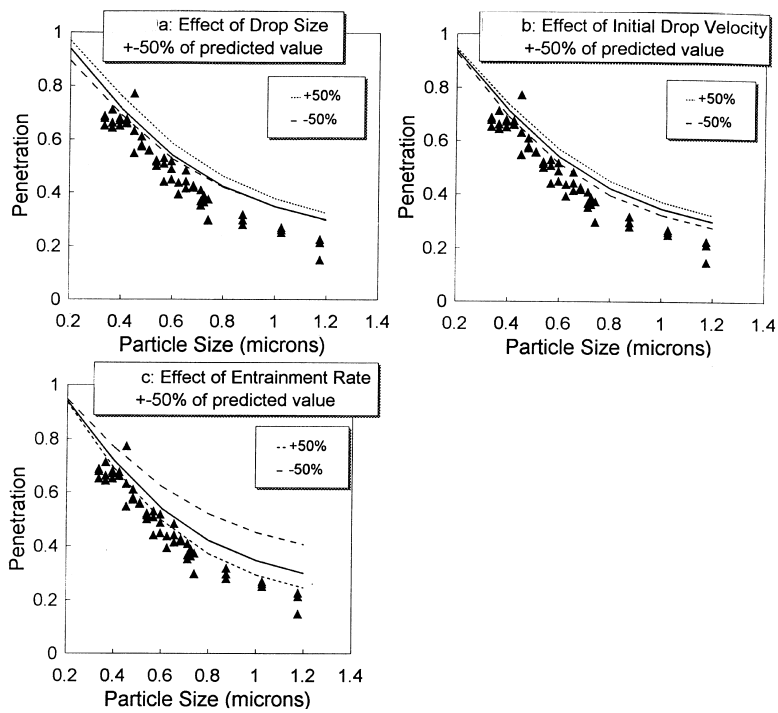

Fig. 9. Effect of model parameters on particle penetration data for wetted approach venturi from Rudnick et al. [3]. Gas flow = 0.1984 kg/s, liquid flow = 0.2216 kg/s.

to 10% of the gas velocity as this was observed by Azzopardi [17] to be the approximate velocity of the waves on a liquid film in annular flow. Fig. 9(c) shows the entrainment rate from the wall film to be an important parameter. The entrainment and deposition from and to the wall uses the method proposed by Whalley and Hewitt [18] for annular flow in pipes, extra entrainment at the beginning and end of the throat is included using the equation suggested by Azzopardi and Govan [8] which considers the component of film velocity towards the centre after the change in wall angle. Koehler et al. [19] have made measurements on the fraction of liquid flow entrained along a venturi (54 mm throat diameter) with

the liquid entering at the start of the throat through a slot and onto the wall of the venturi. Comparison of results for the entrained fraction from the venturi model of Azzopardi et al. [2] show that the model overestimates the entrained flow by 2–3 times. Further investigation of the liquid flows in the film and gas are required to improve model performance.

5. Conclusions

The model of Azzopardi et al. [2] has been shown to give good agreement with available pressure drop data for venturis using both wetted approach and liquid injection at the throat. Extending this model to include particle collection in the venturi, based on the inertial mechanism only, gives significantly improved prediction of dust removal, compared with previous models, over a wide range of operating conditions, particularly when the accuracy of the experimental data is considered. The model provides a reliable method of venturi scrubber design for optimal performance in terms of pressure drop and dust removal.

Important mechanisms that require further experimental investigation to improve the model include drop size and entrainment at liquid injection and entrainment and deposition from the liquid film along the venturi, including any extra entrainment that may take place at the entry and exit to the throat.

6. Nomenclature

c	Dust concentration
C_c	Cunningham correction factor to Stokes Law for particle slip between gas molecules, dimensionless
d	Particle diameter
D	Drop diameter
D_o	Liquid injection orifice diameter
g	Acceleration due to gravity
G	Gas flow (kg/s)
L	Liquid flow (kg/s)
Re_D	Drop Reynolds number ($D\,\rho_g\,u/\mu$)
Re	Reynolds number based on orifice diameter ($D_o\,\rho_l\,v/\mu_1$)
Stk	Stokes number defined by Eq. (1)
u	Relative velocity between gas and drop
v_D	Drop velocity
v_g	Gas velocity
We	Weber number based on orifice diameter ($D_o\,\rho_g v^2/\sigma$)
We_m	Modified Weber number ($\lambda\,\rho_l\,v^2/\sigma$)
W_E	Entrained liquid mass flow rate
W_g	Gas mass flow rate
z	Distance along venturi
η	Collection efficiency
η_i	Inertial collection efficiency
η_p	Inertial collection efficiency in potential flow
η_v	Inertial collection efficiency in viscous flow
λ	Taylor length scale ($\sqrt{(\sigma/g\rho_l)}$)
μ	Gas viscosity
μ_l	Liquid viscosity
ρ_g	Gas density
ρ_l	Liquid density
ρ_p	Particle density
σ	Surface tension

Appendix A. Model equations of Azzopardi et al. [2]

This model assumes that drops travel mainly in the gas core. Drops are deemed to pass through the boundary layer only when they are entrained or when the are on their way to the film to deposit. In the convergent and throat sections, the boundary layer is assumed to be negligibly thin. Boundary layer growth is calculated in the diffuser section by means of a momentum integral approach. The model also calculates the rates of entrainment of liquid as drops and their re-deposition on to the wall film.

The momentum integral equations are a modified version of those developed by Ghose and Kline [20], Bardina et al. [21], Lyrio et al. [22] and Ferziger et al. [23]. The main changes for two phase application are: (i) allowing for the additional effect of the drops in considering the momentum of the core and (ii) the film acting as a rough wall to the gas. The momentum integral equation for boundary layer flow in conical diffusers can be written as

$$\frac{d\theta}{dx}+[2\theta+\delta^*-\delta(1-\xi)]\,\frac{1}{U_\infty}\frac{dU_\infty}{dx} -\frac{\delta}{U_\infty^2}\frac{1}{\rho_g}\frac{dp}{dx}+\frac{\theta}{R}\frac{dR}{dx}=\frac{\tau_w}{\rho_g U_\infty^2}=\frac{C_f}{2} \quad (1')$$

where the term ξ, suggested by Baldina et al. [21], allows for the effects of asymmetry in the flow caused by separation on one part of the diffuser circumference. The pressure gradient is obtained from the contributions of the gas and droplet groups in the core:

$$-\frac{dP}{dx}=\frac{W_g}{A}\frac{dU_\infty}{dx}+\sum_{i-1}^{n}\frac{W_{lEi}}{A}\frac{dU_{Di}}{dx} \quad (2')$$

The gas entrainment equation, which describes the rate at which the inviscid core fluid is entrained into the boundary-layer, for conical geometries takes the form:

$$\frac{1}{RU_\infty}\frac{d}{dx}[RU_\infty(\delta-\delta^*)]=E_{bl} \quad (3')$$

In addition, the equation of continuity for the core can be written as:

$$\frac{1}{U_\infty}\frac{dU_\infty}{dx}=\frac{2}{(1+B)}\frac{dB}{dx}-\frac{2}{R}\frac{dR}{dx} \quad (4')$$

The velocity profile equation used is a modified form of the Coles 'wall-wake' velocity profile which allows for the film acting as a rough surface to the gas:

$$U=\frac{U_\tau}{\kappa}\ln\left(\frac{y}{\epsilon}\right)-8.5U_\tau+\frac{U_\beta}{2}\left[1-\cos\left(\frac{\pi y}{\delta}\right)\right] \quad (5')$$

As explained by Bardina et al. [21], the non-dimensional variables, Λ and h are related by the velocity profile, Eq. (5′), in an approximate linear form which can be used as a shape-factor correlation:

$$h=1.5\Lambda+0.179V_\mathrm{T}+0.321\frac{V_\mathrm{T}^2}{\Lambda} \quad (6')$$

where V_T is obtained by integrating the Coles' velocity profile equation over the boundary-layer:

$$V_\mathrm{T}=\frac{1-2\Lambda}{\left[\ln\left(\frac{\mathrm{Re}^*}{\Lambda}\right)-\ln(\mathrm{Re}_\epsilon)+1.485\right]} \quad (7')$$

After eliminating the pressure gradient term in Eqs. (1′) and (2′), the resulting equations can be combined with the shape-factor correlation, Eq. (6′), and the skin-friction correlation, Eq. (7′) and after appropriate substitutions ($\mathrm{d}V_\mathrm{T}/\mathrm{d}x$ and $\mathrm{d}h/\mathrm{d}x$) and simplifications, a final system of two ordinary differential equations is obtained.

$$a_{11}\frac{\mathrm{d}B}{\mathrm{d}x}+a_{12}\frac{\mathrm{d}\Lambda}{\mathrm{d}x}=b_1 \quad (8')$$

$$a_{21}\frac{\mathrm{d}B}{\mathrm{d}x}+a_{22}\frac{\mathrm{d}\Lambda}{\mathrm{d}x}=b_2 \quad (9')$$

The coefficients of which are:

$$a_{11}=\frac{1-h+C_2(1-B)+B\left(5-3h+2\frac{\xi}{\Lambda}\right)}{B(1-B)}$$

$$a_{12}=-C_1 \quad (10')$$

$$a_{21}=\frac{(1+B)}{(1-B)}\quad a_{22}=-\frac{B}{\Lambda(1-\Lambda)} \quad (11')$$

$$b_1=\frac{\frac{C_\mathrm{f}}{2}}{BR}+\frac{2\left(2-h+\frac{\xi}{\Lambda}\right)-C_2}{R}\frac{\mathrm{d}R}{\mathrm{d}x}$$

$$-\frac{1}{\Lambda}\frac{1}{\rho_\mathrm{g}U_\infty^2}\sum_{i=1}^{n}\frac{W_{\mathrm{lE}i}}{A}\frac{\mathrm{d}U_{\mathrm{D}i}}{\mathrm{d}x}\quad b_2=\frac{\Lambda E_\mathrm{bl}}{R(1-\Lambda)} \quad (12')$$

with

$$C_1=\left[1.5-0.321\left(\frac{V_\mathrm{T}}{\Lambda}\right)^2\right]+\left(0.179+0.462\frac{V_\mathrm{T}}{\Lambda}\right)$$

$$\times\left(\frac{V_T}{\Lambda}-2\right)\left[\ln\left(\frac{\mathrm{Re}^*}{\Lambda}\right)-\ln(\mathrm{Re}_\epsilon)+1.485\right]^{-1} \quad (13')$$

$$C_2=\frac{V_\mathrm{T}}{\left[\ln\left(\frac{\mathrm{Re}^*}{\Lambda}\right)-\ln(\mathrm{Re}_\epsilon)+1.485\right]}$$

$$\times\left(0.179+0.642\frac{V_\mathrm{T}}{\Lambda}\right) \quad (14')$$

To close the system of equations the entrainment parameter, E_bl, is calculated from a simple correlation which was presented by Ferziger et al. [23], and is specially designed for diffuser flows:

$$E_\mathrm{bl}=0.0083(1-\Lambda)^{-2.5} \quad (15')$$

Although this agrees well with experimental data for unstalled or diffusers with small regions of stall, it is not so accurate for detached flows. To overcome these problems, Bardina et al. [21] introduced two physical limits on E_bl after detachment, requiring that (1) U_∞ can never increase in the diffusing section and (2) C_f can never increase in the diffusing section.

Changes in liquid distribution between film and drops are calculated by a mass balance on an element of liquid film:

$$\frac{\mathrm{d}W_\mathrm{lF}}{\mathrm{d}x}=2\pi R(D-E) \quad (16')$$

Following the work of Whalley and Hewitt [18], E is specified by

$$E=kc_\mathrm{E} \quad (17')$$

where k, a mass transfer coefficient, is a function of surface tension and c_E, the equivalent concentration, is a function of a modified Weber number $\mathrm{We}_\mathrm{E}=\tau_i m/\sigma$). At the start of the throat there is assumed to be extra entrainment because the liquid travelling along the convergence is trying to carry on inwards although the wall has changed direction. The equation suggested by Azzopardi and Govan [8] is used:

$$E'=\left(\frac{\tan\theta'}{1+\tan\theta'}\right)\left(\frac{W_\mathrm{lF}-W_\mathrm{lFC}}{2\pi R\Delta x}\right) \quad (18')$$

where W_lFC is given by

$$W_\mathrm{lFC}=\pi R(\nu_\mathrm{l}\rho_\mathrm{l})^{0.5}(\sigma d_\mathrm{t}\rho_\mathrm{l})^{0.25} \quad (19')$$

Deposition is calculated using the approach of Whalley and Hewitt [18]:

$$D=kc \quad (20')$$

The changes in drop velocity are calculated through the acceleration equation using a simple drag law and neglecting all other forces:

$$\frac{\mathrm{d}U_{\mathrm{D}i}}{\mathrm{d}x}=0.75C_{\mathrm{D}i}\frac{\rho_\mathrm{g}}{\rho_\mathrm{l}}\frac{(U_\infty-U_{\mathrm{D}i})\,|U_\infty-U_{\mathrm{D}i}|}{d_{\mathrm{D}i}U_{\mathrm{D}i}} \quad (21')$$

Drop size is specified as a Sauter mean diameter by an equation appropriate to the manner of creation. For drops

produced by the shearing action of the gas on the wall film, an equation suggested by Azzopardi [16] is used

$$\frac{d_{32}}{\lambda_T}=\frac{15.4}{We^{0.58}}+\frac{3.5\rho_g W_{lE}}{\rho_l W_g} \qquad (22')$$

This equation was derived from data taken with annular two-phase flow in vertical pipes.

A.1. Notation for Appendix

A	Local cross-sectional area of the diffuser (m^2)
B	Blockage ($=\delta^*/R$) ($-$)
c	Drop concentration (kg/m^3)
C_D	Drag coefficient ($-$)
C_f	Skin-friction coefficient ($-$)
d_{32}	Sauter mean diameter (m)
d_D	Droplet diameter (m)
d_t	Local diameter of channel (m)
D	Flux of liquid deposition (kg/m^2s)
E	Flux of liquid entrainment (kg/m^2s)
E_{bl}	Boundary-layer gas entrainment rate
h	Shape factor ($=1-\theta/\delta^*$) ($-$)
k	Deposition or entrainment mass transfer coefficient (m/s)
p	Pressure (N/m^2)
R	Local diffuser radius (m)
Re^*	Displacement thickness Reynolds number ($=U_\infty\delta^*/\nu$) ($-$)
Re_ϵ	Reynolds number based on roughness ($=U_\infty\epsilon/\nu$) ($-$)
U	Velocity (m/s)
U_β	Wake amplitude (m/s)
U_τ	Shear velocity (m/s)
U_D	Droplet velocity (m/s)
U_∞	Mean velocity of the core (m/s)
V_T	Non-dimensional shear velocity ($=U_\tau/\kappa U_\infty$) ($-$)
W_g	Gas flow rate (kg/s)
W_{lE}	Entrained liquid flow rate (kg/s)
W_{IFC}	Liquid film flow rate at start of entrainment (kg/s)
W_{IF}	Liquid flow rate in wall film (kg/s)
We	Modified Weber number ($=\rho_l U_\infty^2\lambda_T/\sigma$) ($-$)
We_E	Modified Weber number for entrainment ($=\tau_i m/gs$) ($-$)
x	Axial distance (m)
y	Distance normal to the diffuser wall (m)

Greek letters

δ	Boundary-layer thickness (m)
δ^*	Boundary-layer displacement thickness (m)
ϵ	Roughness parameter (m)
θ	Boundary-layer momentum thickness (m)
θ'	Half angle of convergence (°)
κ	Von Karman constant ($=0.41$) ($-$)
λ_T	Taylor length scale ($=\sqrt{(\sigma/g\rho_l)}$)
Λ	Boundary-layer blockage fraction ($=\delta^*/\delta$) ($-$)
ν	Kinematic viscosity (m^2/s)
ρ	Density (kg/m^3)
σ	Surface tension (kg/s^2)
τ_i	Shear stress at gas/film interface (N/m^2)
τ_w	Wall shear stress (N/m^2)

Subscripts

i	ith group of drops
l, g	Liquid or gas property

References

[1] J.C.F. Teixeira, S.F.C. Teixeira, B.J. Azzopardi, CROCUS, Italy, September 1994.
[2] B.J. Azzopardi, S.F.C. Teixeira, A.H. Govan, T.R. Bott, Trans. Inst. Chem. Eng. 69 (1991) 237.
[3] S.N. Rudnick, J.L.M. Koehler, K.P. Martin, D. Leith, D.W. Cooper, Environ. Sci. Technol. 20 (1986) 237.
[4] S.-C. Yung, S. Calvert, M. Duncan, J. Air Pollut. Contr. Assoc. 34 (1984) 736.
[5] S. Ripperger, G. Dau, Verfahrenstechnik 14 (1980) 164.
[6] S.-C. Yung, S. Calvert, H.F. Barbarika, L.E. Sparks, Environ. Sci. Technol. 12 (1978) 456.
[7] R.H. Boll, Ind. Eng. Chem. Fundam. 12 (1973) 40.
[8] B.J. Azzopardi, A.H. Govan, Filtrat. Separat. 3 (1984) 196.
[9] S. Calvert, AIChE. J. 16 (1970) 392.
[10] I. Langmuir, J. Meteorol. 5 (1948) 175.
[11] H. Herne, The Aerodynamic Capture of Particles, Pergamon, Oxford, 1960.
[12] R.A. Pulley, J.K. Walters, J. Aerosol. Sci. 21 (1990) 733.
[13] W.H. Walton, A. Woolcock, Int. J. Air Pollut. 3 (1960) 129.
[14] S. Nukiyama, Y. Tanasawa, Trans. Soc. Mech. Eng. 5 (1939) 63.
[15] R.D. Ingebo, ICLASS, London, July 1985.
[16] B.J. Azzopardi, Exp. Fluid. 3 (1985) 53.
[17] B.J. Azzopardi, Nucl. Eng. Des. 92 (1986) 121.
[18] P.B. Whalley, G.F. Hewitt, UKAEA report AERE R-7187, 1978.
[19] J.L. Koehler, H.A. Feldman, D. Leith, Aerosol Sci. Tech. 7 (1987) 15.
[20] S. Ghose, S.T. Kline, Trans. ASME, J. Fluids Eng. 100 (1978) 419–426.
[21] J.G. Bardina, A.A. Lyrio, S.J. Kline, J.H. Ferziger, J.P. Johnston, (1981)Trans. ASME, J. Fluids Eng. 103 (1981) 315–321.
[22] A.A. Lyrio, J.H. Ferziger, S.J. Kline, Report PD-23, Dept. of Mechanical Engineering, Stanford University, Stanford, 1981.
[23] J.H. Ferziger, J.H., Lyrio, A.A., Bardina, J.G. (1982), Trans. ASME, J. Fluids Eng., (Vol. 104), 537–540.